

ICASE

SIMULATION OF INSTABILITIES AND SOUND RADIATION IN A JET

Alvin Bayliss

and

Lucio Maestrello

(NASA-CR-185788) SIMULATION OF
INSTABILITIES AND SOUND RADIATION IN A JET
(ICASE) 36 p

N90-70388

00/71 0224383
Unclas

Report No. 81-8
February 8, 1981

INSTITUTE FOR COMPUTER APPLICATIONS IN SCIENCE AND ENGINEERING
NASA Langley Research Center, Hampton, Virginia

Operated by the

UNIVERSITIES SPACE



RESEARCH ASSOCIATION

SIMULATION OF INSTABILITIES AND SOUND RADIATION IN A JET

Alvin Bayliss

Courant Institute of Mathematical Sciences, New York University
New York, NY

and

Lucio Maestrello

NASA Langley Research Center
Hampton, VA

ABSTRACT

The inflow and near-field of a jet which is excited by an axial mass source located in the potential core are simulated numerically. The simulation takes into account the spreading of the jet. Comparison is made with experimental results for both excited and unexcited jets. It is shown that many of the features observed experimentally are due to the instability of the mean profile (i.e. the large scale structures) and not due to the turbulence. This instability is shown to generate low frequency sound. The terms identified by Ribner as the shear noise terms are shown to be responsible for this sound generation.

This work was supported under NASA Contracts No. NAS1-14472 and NAS1-15810 while the first author was in residence at the Institute for Computer Applications in Science and Engineering, NASA Langley Research Center, Hampton, VA 23665.

I. Introduction

This paper is concerned with the effect of a jet flow on an embedded acoustic source. It is primarily a numerical investigation of the full Euler equations linearized about a realistic, spreading axisymmetric jet. The source is modelled by a mass source located along the axis of the jet and downstream of the jet exit. The source is assumed to have a pulse-like behavior in time so that a broadband frequency spectrum can be investigated.

The numerical simulation is computed in a computational domain which includes both the in-flow, near and far-fields. It is thus possible to compute both in-flow instabilities and far-field sound and to study the interaction between them. The simulation has no mechanism to resolve the fine grained turbulence.

In a previous paper the far-field sound was studied. It was shown both experimentally and numerically that an acoustic source placed in a jet had an increase in power output due to the flow. This paper is concerned with an investigation of the near field under the same circumstances as the earlier far-field study.

Many authors have observed large scale orderly structures in the flow field of a jet. Crow and Champagne² and Moore³ investigated this structure in excited jets and related it to the instability of the mean jet profile. Maestrello and Fung⁴ measured the fluctuating pressure just outside the boundary of an unexcited jet. They found a low frequency, axisymmetric structure which peaks at roughly three diameters downstream of the nozzle and decays further downstream. Similar disturbances were observed by Chan.⁵ Tam⁶ demonstrated analytically that an acoustic source could excite instability waves in a supersonic jet.

Vlasov and Ginevsky reported a large amplification in the fluctuating velocity when they excited the jet by an acoustic disturbance. Their results

*Category: Jet Noise

did not indicate whether the resultant increase was due to a large scale structure or small scale turbulent fluctuation. Zaman and Hussain⁸ excited the jet upstream of the nozzle and found a large increase in the time averaged Reynold's stresses.

Michalke⁹ has shown that instability waves of infinite extent, such as those obtained by a parallel flow approximation can not generate sound. In a realistic jet spatial, instability waves grow exponentially and then decay due to the spread of the jet and the thickening of the shear layer. In general the lower frequencies peak further downstream. Liu¹⁰ computed instability waves in a free shear layer, by using parallel flow theory together with an axially varying shape function which satisfied an energy propagation equation. Tam and Morris¹¹ have recently used a multiple scale analysis to demonstrate that instability waves in a spreading, free shear layer generate far-field sound.

Experimental results presented by McLaughlin, et al.¹² indicated that instability waves generate sound in low Reynold's number supersonic jets. Numerical and experimental results presented in reference 1 indicated that the far-field sound produced by an axial source was amplified when the source was placed in a jet. It was further shown that the maximum amplification occurred at the frequency which was most unstable at the position of the source. This strongly suggested that the amplification was due to sound generation by instability waves. Bechert and Pfizenmaier¹³ also measured an increase in far-field power when the jet was excited upstream of the nozzle.

In this paper the generation of sound by instability waves will be explicitly demonstrated by examination of near-field data. In addition, the generation of large scale structures and their temporal evaluation will be

studied. It will also be shown that many of the qualitative features observed experimentally in the flow field and near-field of both excited and unexcited jets can be described by linear instability theory.

The results will also demonstrate that the specific terms responsible for destabilizing the flow are analagous to the shear noise terms identified by Ribner^{14,15} and others (see Doak⁶) based on the general source term in the Lighthill¹⁷ analogy. Many authors have tried to modify the Lighthill theory to account for propagation through a mean flow. Since the Lighthill equation is in principal exact, this requires identifying the propagation operator (i.e., left hand side) and the sources (right hand side) which must necessarily be modelled. The formulation of Phillips¹⁸ led to a convective wave equation which neglected these shear noise terms. The subsequent formulation by Lilly¹⁹ led to a third order equation which accounted for all first order interactions between the fluctuating and mean fields. Ribner¹⁴ pointed out that the shift of the shear terms from source terms to the left hand side was an essential step in obtaining Lilley's equation. He further showed that the shear terms were an important component of the low frequency part of the spectra.

Computations with Lilly's equation were performed by Tester and Morfrey.²⁰ These computations were based on the parallel flow approximation and were thus unable to simulate the generation of sound by instability waves. Schubert²¹ and Maestrello and Liu²² computed with a Phillip's type convective wave equation in a spreading jet and were thus unable to trigger the instability of the mean flow. The results presented here exhibit the shear noise terms as those which destabilize the flow and thus generate sound through the action of the large scale structures.

In section 2 the governing equations are introduced and the numerical simulation is discussed. Further details can be found in reference 1. Section 3 contains the results and a discussion of their significance.

II. Theory

We consider the Euler equations in axisymmetric, cylindrical coordinates z and r linearized about mean profiles of the form (U_0, V_0, ρ_0) . Here U_0 and V_0 are the mean axial and radial velocity profiles of the jet and ρ_0 is the mean density which for simplicity is assumed constant. The mean profiles were obtained experimentally by Maestrello.²³ This profile has a spread of about 11° from a virtual origin 2.57 diameters upstream of the nozzle exit. If the flow is also assumed to be homentropic the mean sound speed, c_0 is also constant. The fluctuating pressure and velocities (p, u, v) are then the solution to the following system of equations

$$\begin{aligned}
 (a) \quad & p_t + (U_0 p + u \rho_0 c_0^2)_z + (V_0 p + v \rho_0 c_0^2)_r + \frac{V_0 p + v \rho_0 c_0^2}{r} = m, \\
 (b) \quad & u_t + (U_0 u + \frac{p}{\rho_0})_z + (V_0 u)_r - u V_{0,r} + v U_{0,r} = 0, \\
 (c) \quad & v_t + (U_0 v)_z + (V_0 v + \frac{p}{\rho_0})_r - v U_{0,z} + u V_{0,z} = 0.
 \end{aligned} \tag{2.1}$$

The forcing term m corresponds to the time rate of change of an axial source of mass/unit volume which is assumed to dominate the natural sources. This mass source is generally taken to be of the form

$$m(t, \vec{x}) = f(t) \delta(|\vec{x} - \vec{x}_0|),$$

where $f(t)$ is chosen to have the pulse-like form

$$f(t) = e^{-\left(at^2 + \frac{b}{t^2}\right)} \quad t \geq 0,$$

for positive constants a and b . These constants are chosen so that the resultant pulse has a peak at around 1000 Hz. The δ function is approximated by a Gaussian.

The left-hand side of (2.1) includes all of the first order interaction terms between the fluctuating and mean fields and in particular includes the equations governing linear stability theory. In the far-field as U_0 and $V_0 \rightarrow 0$ we can recover the ordinary wave equation governing the propagation of acoustic radiation. The undifferentiated terms on the left-hand side of (2.1b,c) represent the interaction of the fluctuating field with the mean shear. They are large only in the vicinity of the jet shear layer, however it is exactly these terms which initiate the instability of the mean flow.

Formulations which do not allow for these terms can not correctly simulate the near-field. Results presented here and in ref. 1, using numerical experiments whereby these terms are simply switched off, demonstrate that these shear noise terms are also responsible for increases in the far-field sound via the generation of sound from instability waves.

The computational domain is a rectangular region in the r, z plane, with the jet exiting from a constant area pipe upstream of the source (see figure 1). The equations are solved by the method of time splitting using a fourth order discretization in space.^{1,24} The details of the numerical algorithm are described in detail in reference 1. The scheme is of MacCormack type, with fourth accuracy in the spatial variables.²⁴

Boundary conditions at the far-field boundary must simulate outgoing radiation. The appropriate time dependent version of the Sommerfeld radiation condition is

$$\frac{\partial p}{\partial t} + \frac{\partial \tilde{u}}{\partial t} + \frac{p}{\sqrt{r^2 + z^2}} = 0$$

where u is the radial velocity.¹ At the upstream nozzle boundary we impose

$$v = 0$$

$$p + u = 0,$$

valid for low frequency wave propagation down the pipe.¹

The jet has a nozzle diameter (D) of 5.08 cm. The simulations were conducted at an exit Mach number of 0.66, corresponding to a Reynolds number based on diameter of approximately 8×10^5 .

III. Results and Discussion

Results are obtained for the fluctuating pressure and for the velocities in both the broad and narrow band. Numerical results are also obtained with the shear interaction terms in (2.1) formally set to zero. In reference 1 it was found that without these terms there was virtually no far field power amplification for the low frequencies.

The mean flow U_0 will have an inflection point within the shear layer of the jet. As a consequence of this inflection point, U_0 will be linearly unstable. The instability will diminish with downstream distance as the region around the inflection point flattens out. In Figure 3 we plot $\tilde{U} = U_0/U_c$ as well as $\partial \tilde{U} / \partial r$ as a function of r/D at the

downstream station $z/D = 2$. The velocity U_c refers to the center line velocity. The region around the inflection point will become broader further downstream.

The r.m.s. speed $\sqrt{u^2 + v^2}$ is shown in Figs. 3a and 3b as a function of the radial distance r/D , at two downstream locations. The figures show the results with and without flow and with and without the shear interaction terms.

The results with flow show a very strong amplification in the region of the inflection point. The large amplification is consistent with the amplification of the fluctuating velocities measured in references 7 and 23. The measurements in reference 7 were primarily concerned with small scale turbulence, although these measurements must have included the larger scale instability waves.

The velocity amplification exhibits a narrow peak at $z/D = 2$ where the shear layer is very thin. At $z/D = 4.2$ the peak flattens out towards the jet centerline as the shear layer thickens. This behavior is very similar to r.m.s. velocity fluctuations observed experimentally in unexcited jets (see Fig. 4).²² Since the numerical simulation does not include turbulence it is evident that this behaviour is a consequence of the large scale structure. This is further confirmed by the absence of these strong peaks when the destabilizing shear terms are omitted.

We next consider the time averaged Reynold's stressess (\overline{uv}) and extra vorticity $(\frac{\partial u}{\partial r} - \frac{\partial v}{\partial z})$ (multiplied by r) induced by the sound pulse. In Figs. 6a and 6b these quantities are plotted as functions of r/D for the two downstream locations $z/D = 2$ and $z/D = 4.2$. The plots of the pulse-induced vorticity indicate the presence of two vortical regions of opposite sign superimposed on the mean flow vorticity. It can further be

seen that the Reynold's stresses peak near the point of maximum shear and become slightly negative near the jet boundary and near the axis. These numerical plots are likewise typical of experimental results obtained for both excited and unexcited jets (see for example reference 8).

The area under the curves of Figs. 5a and 5b (and other curves of similar shape not shown) is nonzero (negative). This indicates that the integral of the time-average pulse-induced vorticity over the cross-section of the jet is nonzero for these stations. It seems a safe inference that the volume integral of this extra vorticity over the first 6 diameters at least is nonzero. Whether this would be cancelled by an integral of the remainder of the jet remains open. The possibility of creation of extra vorticity by a sound pulse in a jet raises interesting theoretical questions. One mechanism of transient vorticity generation is vortex stretching/compression during passage of the pulse, but this would tend to yield a zero time average.

To further exhibit the relationship between the inflow fluctuating field and spatial instability waves we consider the longitudinal fluctuating velocity in the frequency domain ($\hat{u}(z,r,f)$). Instability waves based on linear spatial stability theory have the functional form

$$\hat{u}(z,r,f) = e^{i\omega t} e^{-i\alpha z} \hat{f}(r) A(z), \quad (3.1)$$

where $\omega = 2\pi f$, $\alpha(z)$ is the wave number computed from stability theory, $f(r)$ is the corresponding eigenfunction and $A(z)$ is a slowly varying amplitude (see reference 10). The jet profile is known to be unstable to axisymmetric low frequency disturbances; thus there always exist solutions that grow along the axis ($\alpha_i \equiv \text{imag. part of } \alpha > 0$).

The solution can be represented as a superposition of time harmonic waves by Fourier transforming the data. In Fig. 6 an approximation to the disturbance growth rate α_1 is obtained by fitting the functional form (3.1) to the data output along the axis $r = 0$ (α_1). The growth rate is plotted at different downstream stations as a function of $St_z = fz/U_j = 0.3$, where U_j is the jet velocity. The peak growth rate occurs at approximately $St_z \sim 0.3$. In reference 1 it is shown that $St_z \sim 0.3$ corresponds to the peak amplification of the far-field acoustic power.

The growth rates plotted in Fig. 6 are qualitatively similar to those obtained by Mattingly and Chang²⁵ using a model profile. The amplification rate peaks at roughly three diameters downstream and decrease as z increases further. Further downstream the helical mode may be the most unstable mode.²⁵ This mode is not present in the numerical simulation because of the axial symmetry.

We next consider the near-field fluctuating pressure. Since measurements of the pressure fluctuations can be most readily interpreted when taken outside of the flow, we compute the near-field pressure fluctuations ratio (power spectrum with flow/power spectrum with no flow) just outside the jet at $z/D = 2, 4.2$, and 6 . The results, when plotted against St_z in Fig. 7 show a peak near $St_z = 0.4$, which is close to the peak computed for the far-field amplification (see reference 1).

In Figure 8 the experimental counterpart is shown as a function of longitudinal Strouhal number St_z for three values of $St_D = fD/U_j$. It is noted that the peak pressure occurs at $St_z \sim 0.6$. In reference 4 this structure is attributed to the instability of the jet. Experimental results with the excited jet reported in reference 1 show the peak far-field spectral amplification occurring near the same Strouhal number $St_z = 0.6$.

To further study the structure of the near field and in-flow field fluctuating pressure, we present contour plots of p as a function of z/D and time t with r/D fixed. Pressure is normalized by the distance $\sqrt{(r/D)^2 + (z/D)^2}$ in order to simplify the interpretation. In Figs. 9a through 9f these plots are given for $r/D = 0, .4, .86, 1.5, 2.3$, and 3.3 . For comparison we present in Fig. 10 a similar plot with $r/D = 0$ for the no flow case.

The interesting feature to observe in these plots is the splitting of the original pulse into two pulses in the presence of the flow. The first pulse can clearly be identified as the acoustic pulse since it travels with a velocity which tends to the ambient sound speed c_0 (normalized to unity in the figure). The actual speed is slightly larger due to convection effects. We note that the pulse is reduced in amplitude from the no flow case (Fig. 10) and is considerably broadened. This is a refraction effect and outside the flow the acoustic field is strongly amplified for the reasons discussed earlier.

The second pulse is much broader and travels with a group velocity proportional to the local mean flow U_0 . The proportionality constant is about 0.7 which is close to the value measured by Crow and Champagne.² After initial growth the pulse decays within the jet and will not reach the far-field. The pulse is much greater than the acoustic pulse for r/D near the inflection point and decays at a very fast rate beyond.

It is evident from the figures that the instability wave is itself split into a leading and a trailing pulse. The initial stages of the pulse formation are very complicated. However, by studying the development of the pulse for different source positions, we have found the trailing part of this wave to be delayed when the source is placed further from the nozzle exit. The leading pulse does not have such a lag. This suggests

that the trailing pulse is generated by interaction with the nozzle while the leading pulse is generated by interaction with the shear layer near the source.* The authors plan to examine the details of this large scale structure in a subsequent publication.

A different view of this large scale structure can be seen in figures 11a, b, c where perspective plots of the fluctuating pressure are shown at a fixed time as a function of r/D and z/D . It is clearly seen that the omission of the shear terms prevents the formation of the instability wave. Figure 11c shows the difference between the two simulations. Comparison between Fig. 11a and 11b clearly indicates the acoustic enhancement due to the instability wave. The generation of sound by the large scale structure is clearly indicated by these results.

IV. Conclusion

The numerical simulation predicts a large amplification of the in-flow fluctuating field in an excited jet. A large scale axisymmetric structure is seen to be generated. This is accompanied by an increase in the far-field acoustic intensity. Both phenomena occur primarily in the low to medium frequency range and have been observed experimental (see ref. 1). There is clear evidence that this amplification is due to the triggering of instability waves by the pulse.

On omitting the shear interaction terms between the fluctuating velocities and the mean flow gradients, the far-field is greatly reduced. Furthermore, the far-field directivity pattern becomes similar to the patterns obtained from an ordinary convective wave equation which are attributed mainly to refraction effects.

* This phenomena was suggested to the authors by Prof. Christopher K. W. Tam.

These flow gradient terms are in effect the shear noise source terms in the Lighthill equation. Ribner¹⁴ showed that the shear noise term is largely responsible for low frequency sound radiation in a jet. The results indicate that this noise is generated by the so-called large scale structures.

The results presented here were obtained by solving a hyperbolic initial value boundary value problem. In ref. 1 a family of boundary conditions were introduced, which enabled the fluctuating field to be computed in a computational domain which is localized in the vicinity of the flow. This suggest that the in-flow data, computed in a relatively small region near the flow can be input into existing theories of aerodynamic noise (e.g. refs. 17, 26) to compute the sound generated by the large scale structures.

Acknowledgment

The authors would like to acknowledge Mr. Stan Lamkin for obtaining most of the computer results discussed in this paper.

References

¹Maestrello, L., Bayliss, A., and Turkel, E., "On the Interaction of a Sound Pulse with the Shear Layer of an Axisymmetric Jet," *Journal of Sound and Vibration*, Vol. 74, No. 1, 1981.

²Crow, S. and Champagne, F., "Orderly Structure in Jet Turbulence," *Journal of Fluid Mechanics*, Vol. 89, 1978, pp. 357-371.

³Moore, C. J., "The Role of Shear-Layer Instability Waves in a Two-Dimensional Shear Layer by Sound," *Journal of Fluid Mechanics*, Vol. 89, 1978, pp. 357-371.

⁴Maestrello, L. and Fung, Y. T., "Quasi-Periodic Structure of a Turbulent Jet," *Journal of Sound and Vibration*, Vol. 64, 1979, pp. 107-122.

⁵Chan, Y. Y., "Noise Generated by Wave-Like Eddies in a Turbulent Jet," *The Tenth Congress of the International Council of the Aeronautical Sciences*, Paper No. 76-42, Ottawa, Canada, October 1976.

⁶Tam, C. K. W., "Excitation of Instability Waves in a Two-Dimensional Shear Layer by Sound," *Journal of Fluid Mechanics*, Vol. 89, 1978, pp. 357-371.

⁷Vlasov, Ye V. and Ginevskiy, A. S., "Generation and Suppression of Turbulence in an Axisymmetric Turbulent Jet in the Presence of an Acoustic Influence," NASA TT-F15, 721, 1974.

⁸Zaman, K. B. M. Q. and Hussain, A. K. M. F., "Vortex Pairing in a Circular Jet under Controlled Excitation," Part I., Report FM-1, Department of Mechanical Engineering, University of Houston, Houston, Texas, November 1978.

⁹Michalke, A., "Sound Generation by Amplified Disturbances in Free Shear Layers," German Air and Space Travel Research Report 69-90, 1969.

¹⁰Liu, J. C., "Developing Large Scale Wave-like Eddies and the Near Jet Noise Field," *Journal of Fluid Mechanics*, Vol. 62, 1974, pp. 437-464.

¹¹Tam, C. K. W. and Morris, P. J., "The Radiation of Sound by the Instability Waves of a Compressible Plane Turbulent Shear Layer," *Journal of Fluid Mechanics*, Vol. 48, Part 2, 1980, pp. 349-381.

¹²McLaughlin, D. K., Morrison, G. L. and Troutt, T. R., "Experiments on the Instability Wave in a Supersonic Jet and Their Acoustic Radiation," *Journal of Fluid Mechanics*, Vol. 69, 1975, pp. 73-95.

¹³Bechert, D. W., Pfizenmaier, E., "On the Amplification of Broad Band Jet Noise by Pure Tone Excitation," *AIAA Journal*, Vol. 15, 1977, pp. 12-68.

¹⁴Ribner, H. S., "On the Role of Shear Noise Term in Jet Noise," *Journal of Sound Vibration*, Vol. 52, 1977, pp. 121-132.

¹⁵Ribner, H. S., "Perspectives on Jet Noise," Dryden Lecture, AIAA 19th Aerospace Sci. Meeting, St. Louis, MO, January 12-15, 1980, AIAA-81-0428.

¹⁶Doak, P. E., "Fundamentals of Aerodynamic Sound Theory and Flow Duct Acoustics," *Journal of Sound and Vibration*, Vol. 28, 1973, pp. 527-561.

¹⁷Lighthill, M. J., "On Sound Generated Aerodynamically - I. General Theory," *Proceedings of the Royal Society A211*, 1952, pp. 564-578.

¹⁸Phillips, O. M., "The Irrotational Motion Outside the Free Turbulent Boundary," *Proceedings of the Cambridge Philosophical Society*, Vol. 51, 1955, pp. 222-229.

¹⁹Lilley, G. M., "Theory of Turbulence Generated Jet Noise: Generation of Sound in a Mixing Region," United States Air Force Technical Report AFAPL-TR-72-53, Vol. IV, 1972.

²⁰Tester, B. J. and Morfrey, C., "Developments in Jet Noise Modelling - Theoretical Predictions and Comparison with Measured Data, *Journal of Sound and Vibration*, Vol. 46, 1976, pp. 79-103.

²¹Schubert, L. K., "Numerical Study of Sound Refraction by a Jet Flow. II. Wave Acoustics," *Journal of the Acoustical Society of America*, Vol. 51, 1972, pp. 439-446.

²²Liu, C. H. and Maestrello, L., "Propagation of Sound Through a Real Jet Flow Field," *AIAA Journal*, Vol. 13, 1975, pp. 66-70.

²³Maestrello, L., "Acoustic Energy Flow from Subsonic Jets and their Mean and Turbulent Flow Structure," Ph.D. Thesis, Institute of Sound and Vibration, 1975.

²⁴Gottlieb, D. and Turkel, E., "Dissipative Two-Four Methods for Time-Dependent Problems," *Mathematics of Computation*, Vol. 30, 1976, pp. 703-723.

²⁵Mattingly, G. E. and Chan, C. C., "Unstable Waves on an Axisymmetric Jet Column, *Journal of Fluid Mechanics*, Vol. 65, Pt. 3, 1974, pp. 541-560.

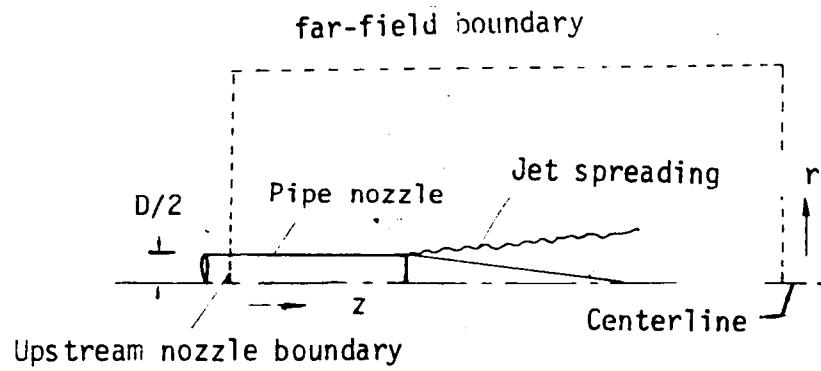


Figure 1. Computational domain

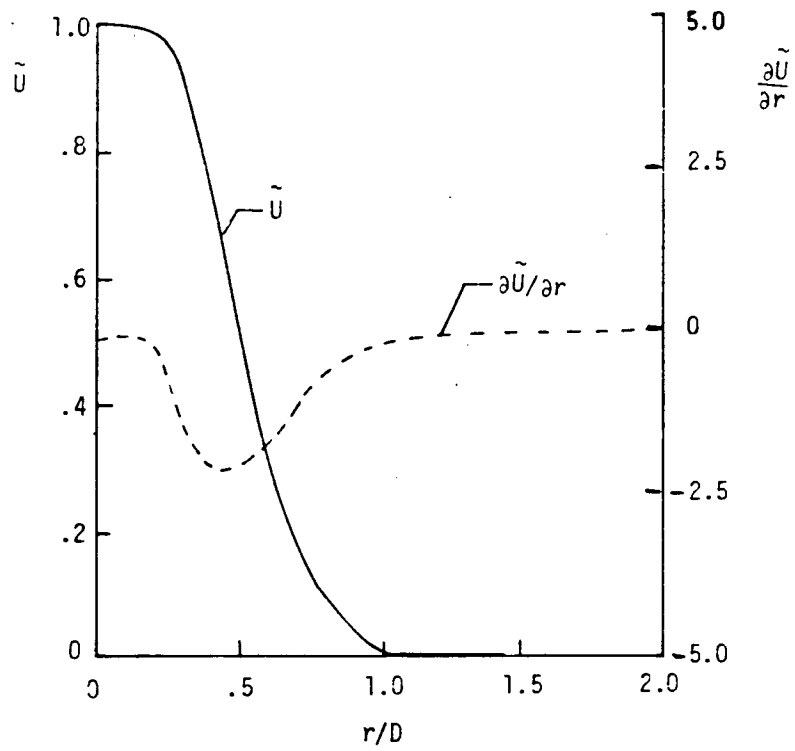


Figure 2. Mean velocity profile and radial derivative at $z/D = 2$.

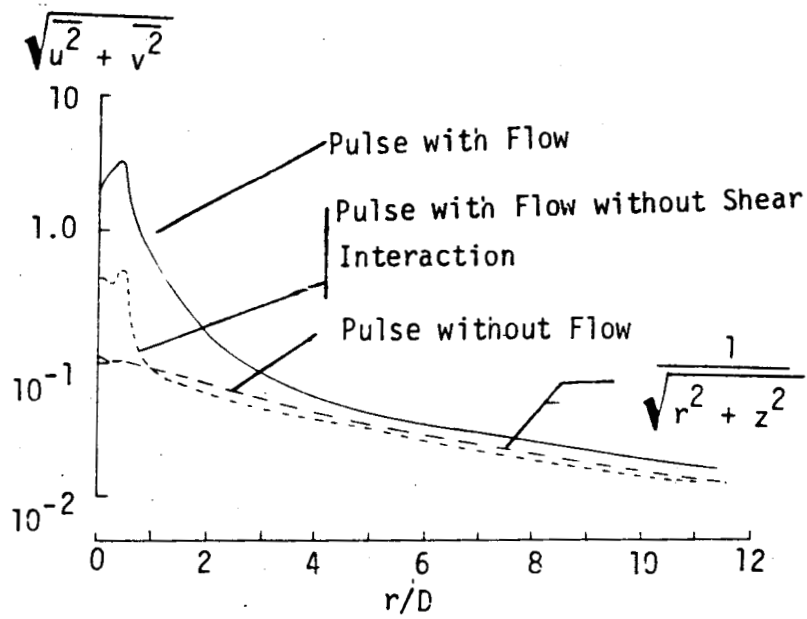


Figure 3a. Normalized R.M.S. velocity across the shear layer at $z/D = 2$.

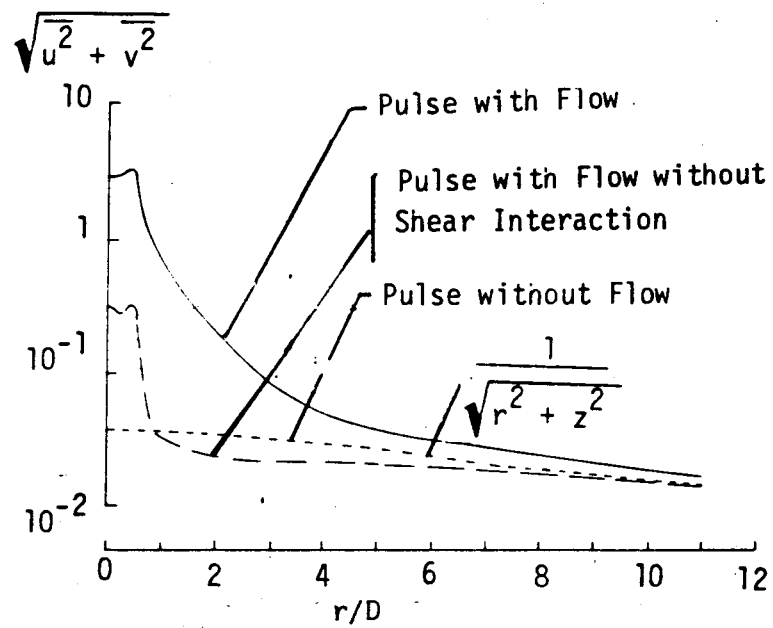


Figure 3b. Normalized R.M.S. velocity across the shear layer at $z/D = 4.2$.

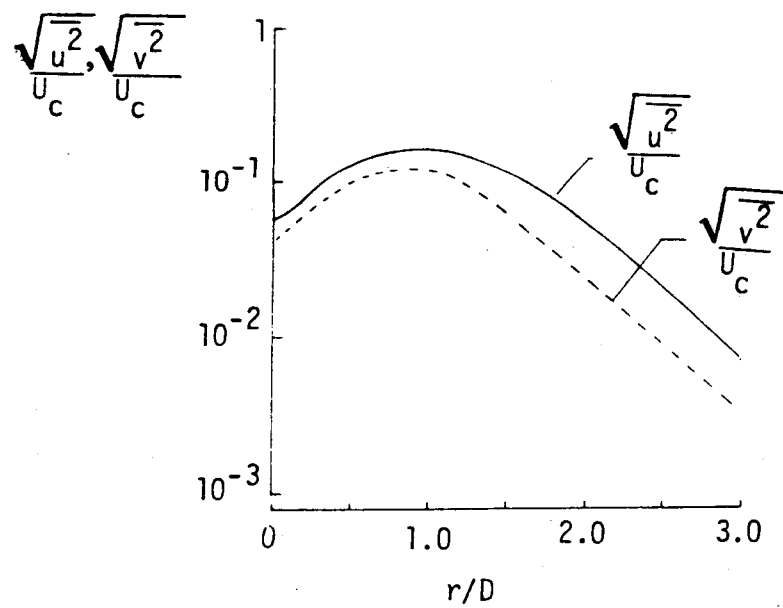


Figure 4. Measurements of the mean fluctuating velocity for the unexcited jet at $z/D = 2.0$.

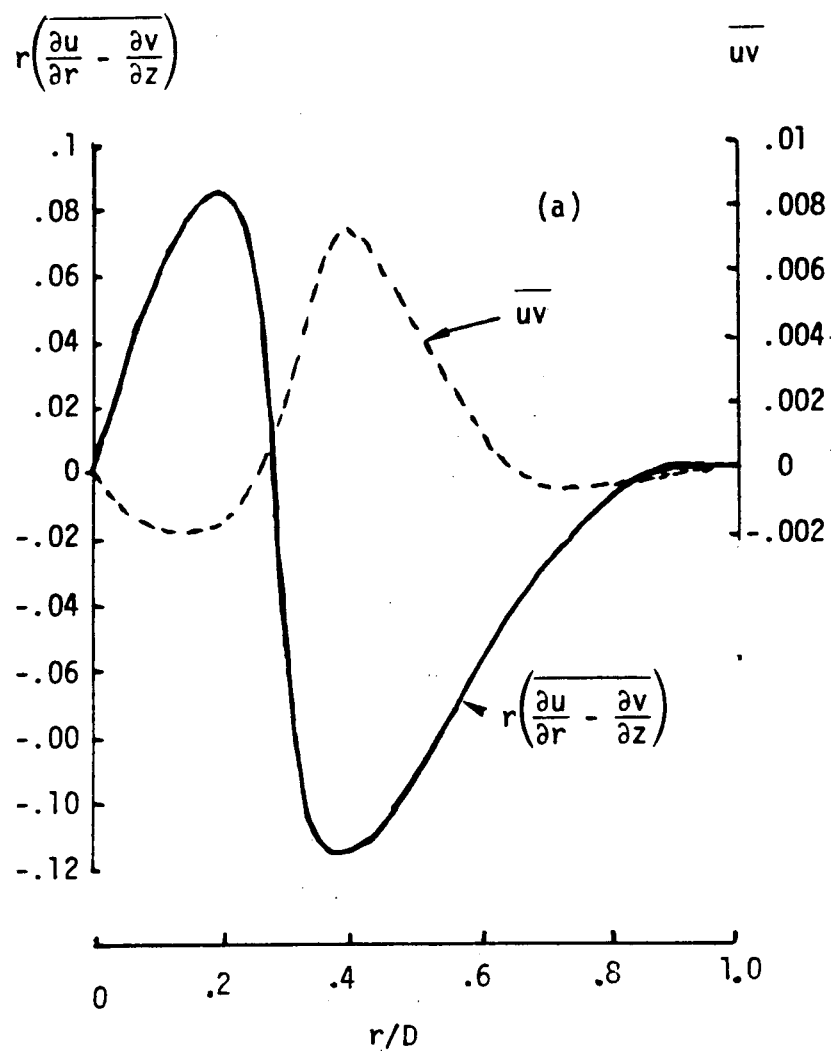


Figure 5a. Normalized time average Reynolds stresses and vorticity. $z/D = 2$.

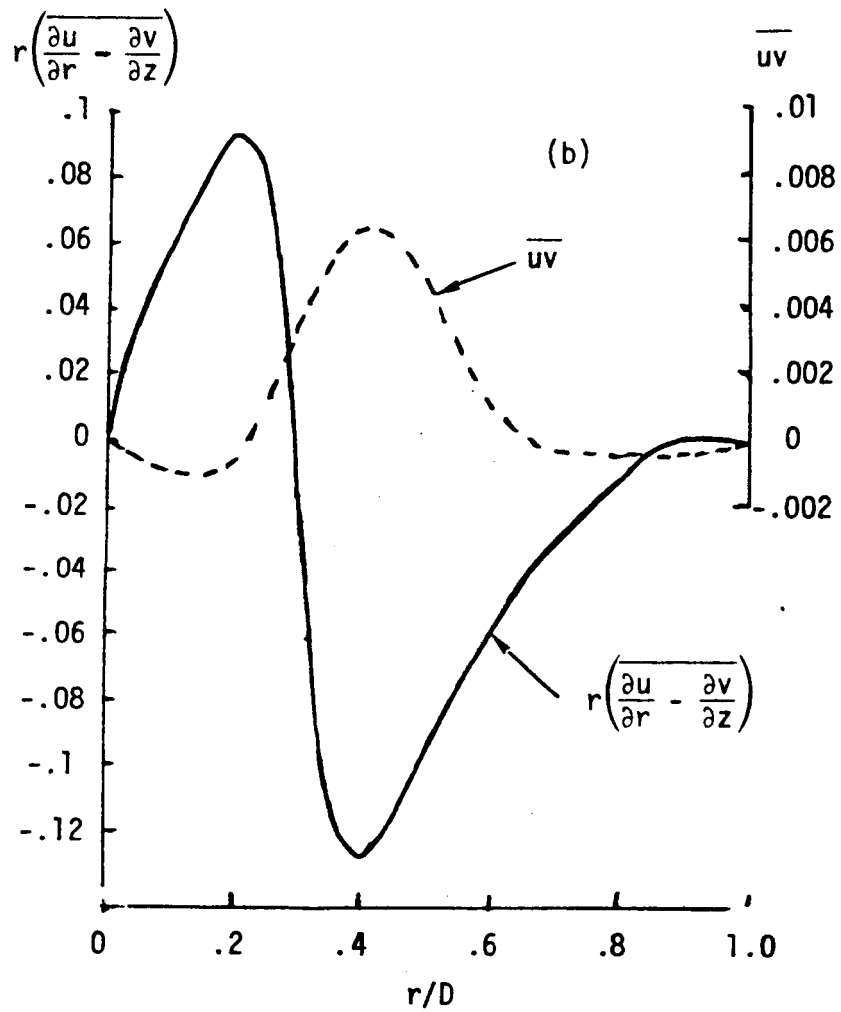


Figure 5b. Normalized time average Reynolds stresses and vorticity. $z/D = 4.2$.

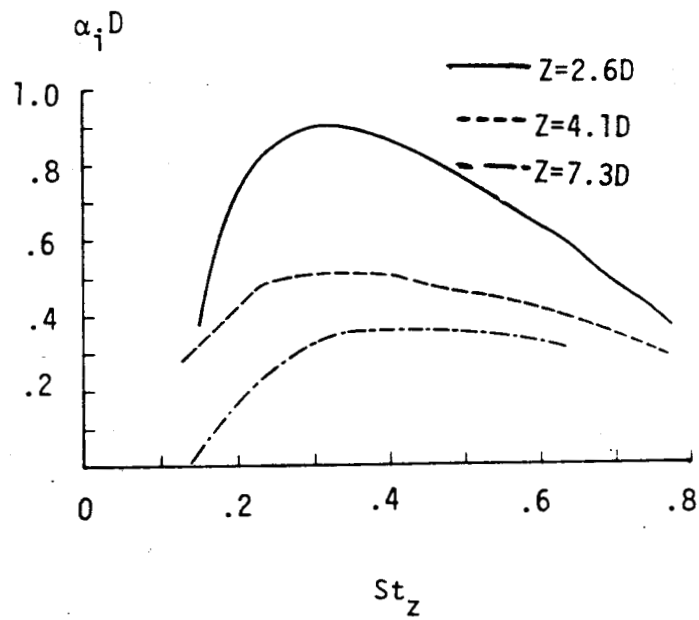


Figure 6. Centerline amplification St_z rate of the longitudinal fluctuating velocity.

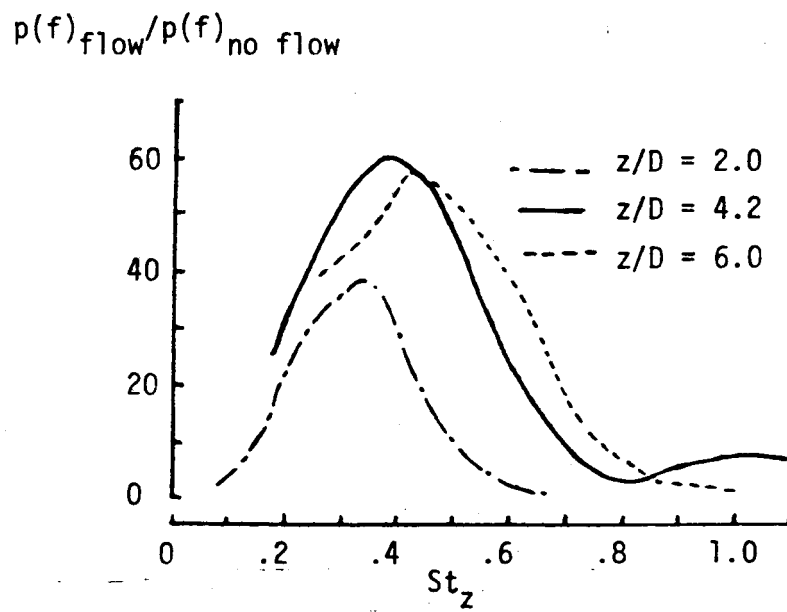


Figure 7. Near-field amplification rate.

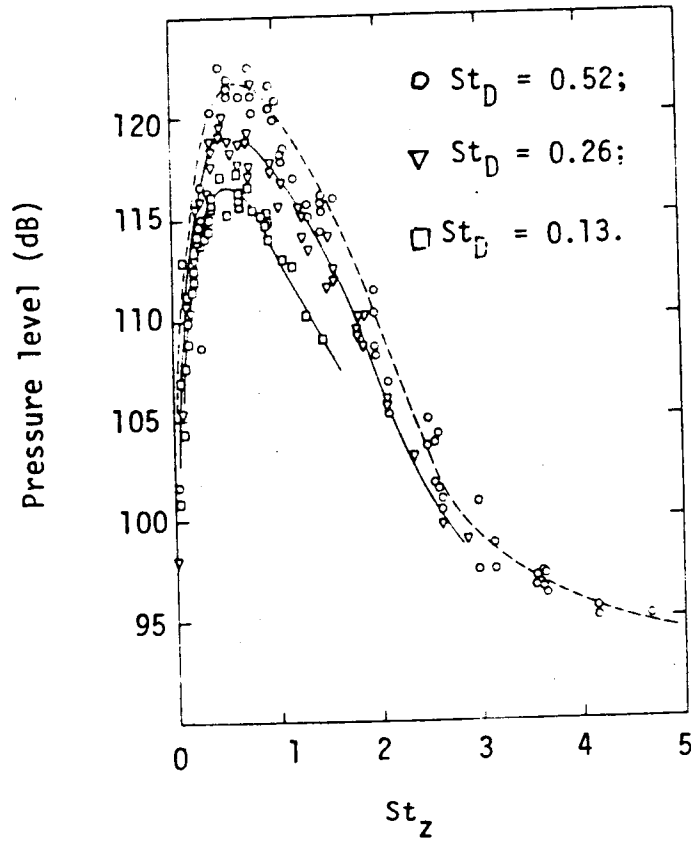


Figure 8. Experimental near-field pressure with downstream distance.

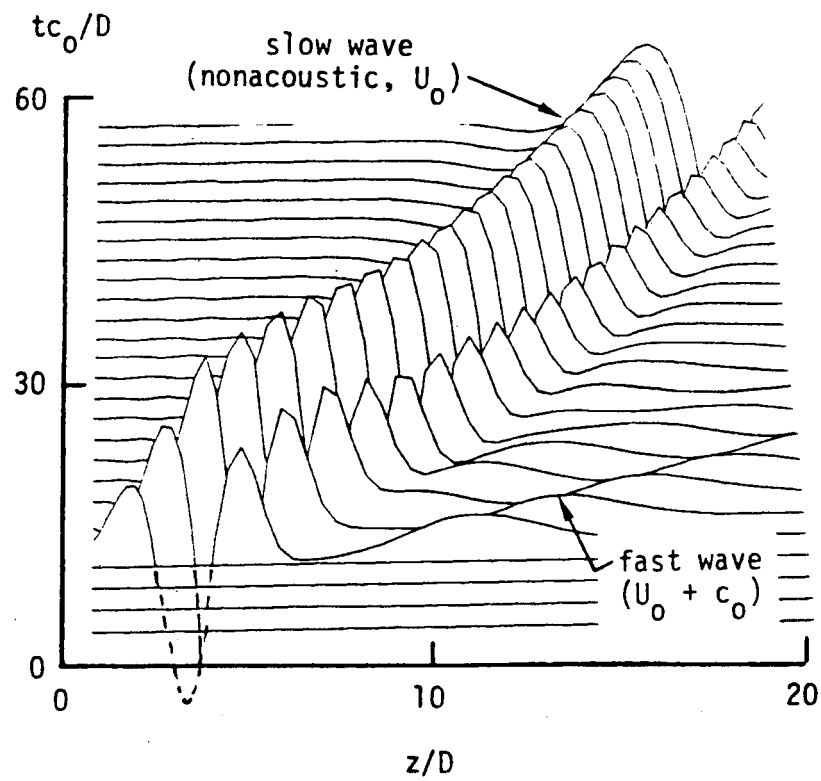


Figure 9a. Three-dimensional prospective of the evolution of the pressure amplitude at $r/D = 0$.

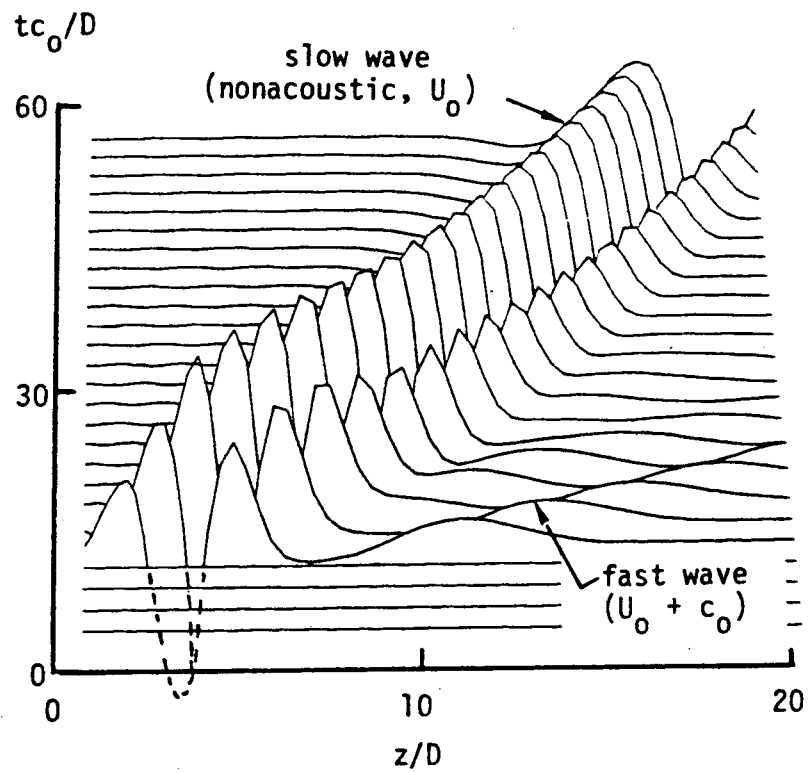


Figure 9b. Three-dimensional prospective of the evolution of the pressure amplitude at $r/D = .4$.

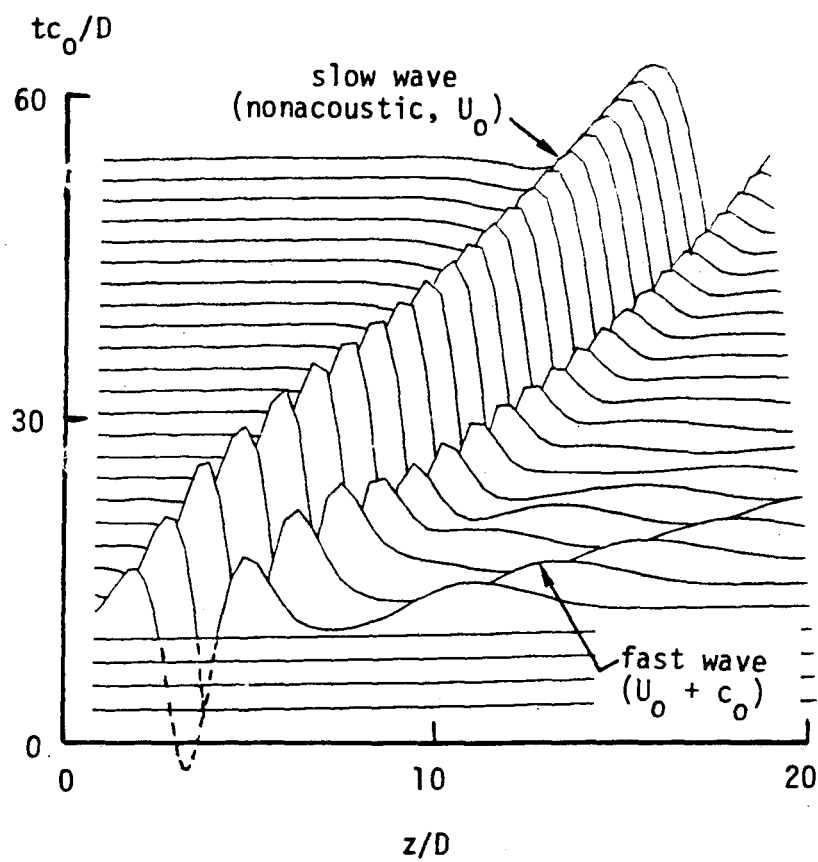


Figure 9c. Three-dimensional prospective of the evolution of the pressure amplitude at $r/D = .86$.

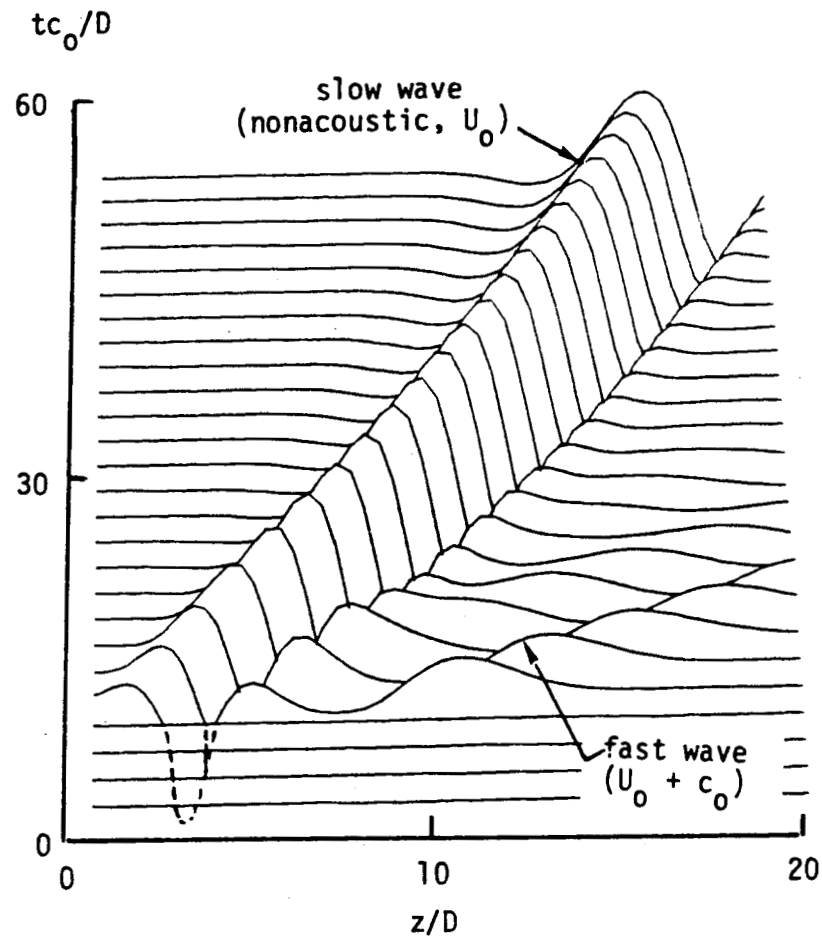


Figure 9d. Three-dimensional perspective of the evolution of the pressure amplitude at $r/D = 1.5$.

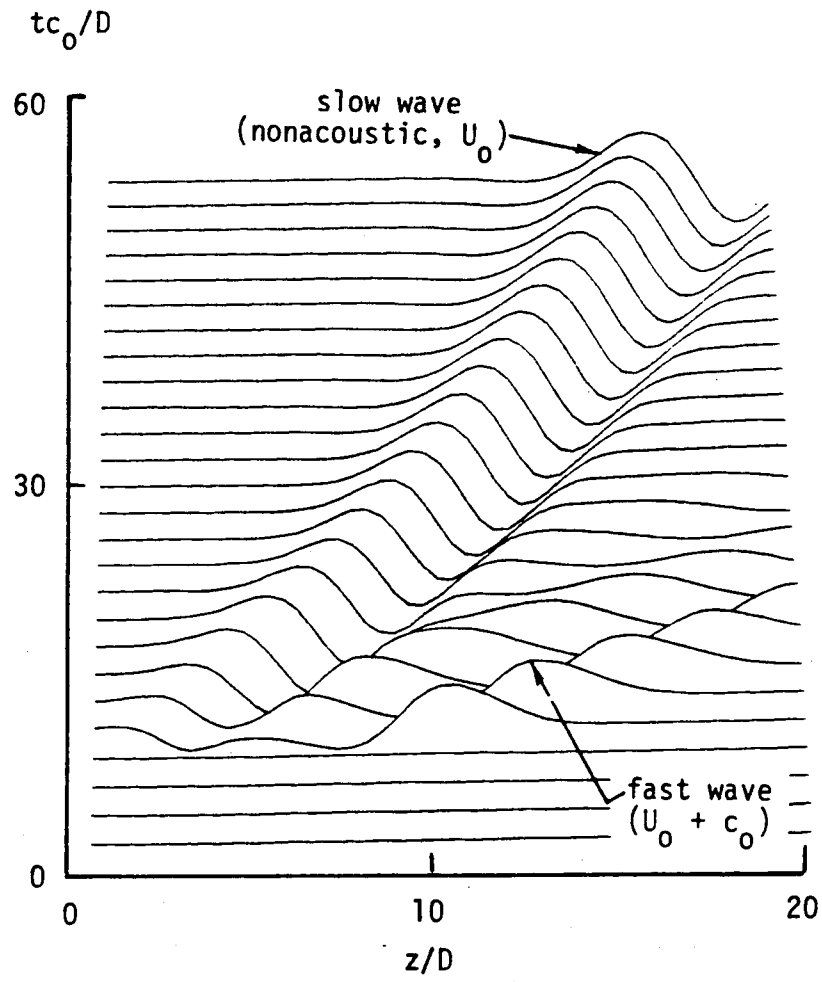


Figure 9e. Three-dimensional prospective of the evolution of the pressure amplitude at $r/D = 2.3$.

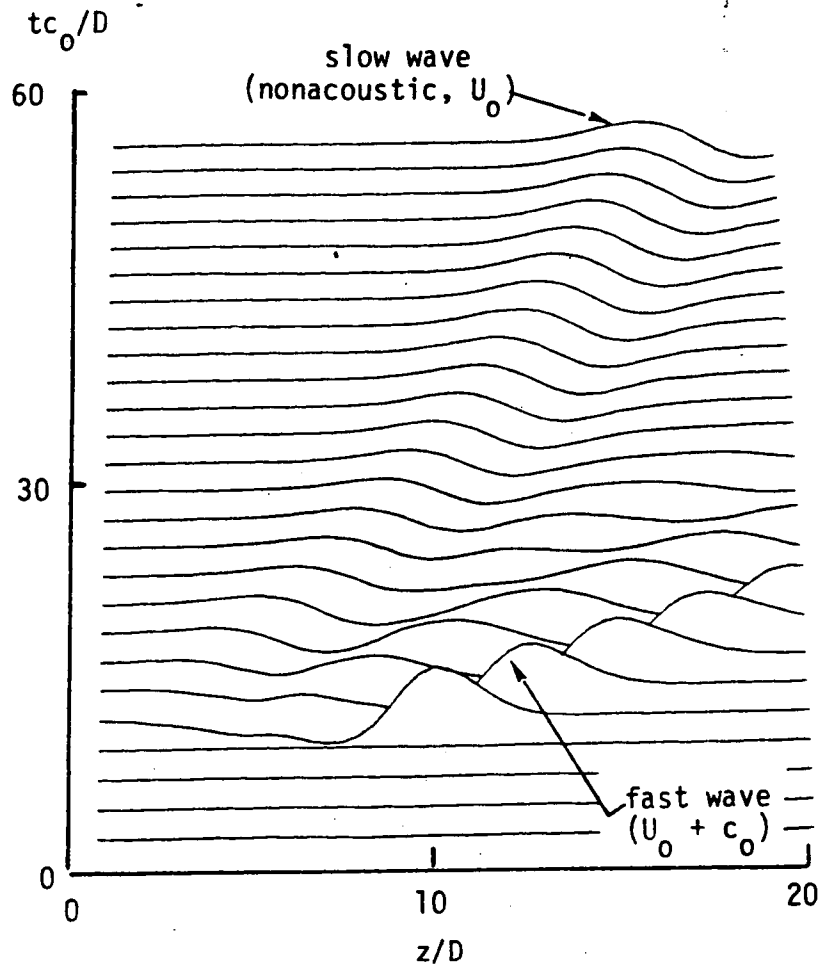


Figure 9f. Three-dimensional prospective of the evolution of the pressure amplitude at $r/D = 3.3$.

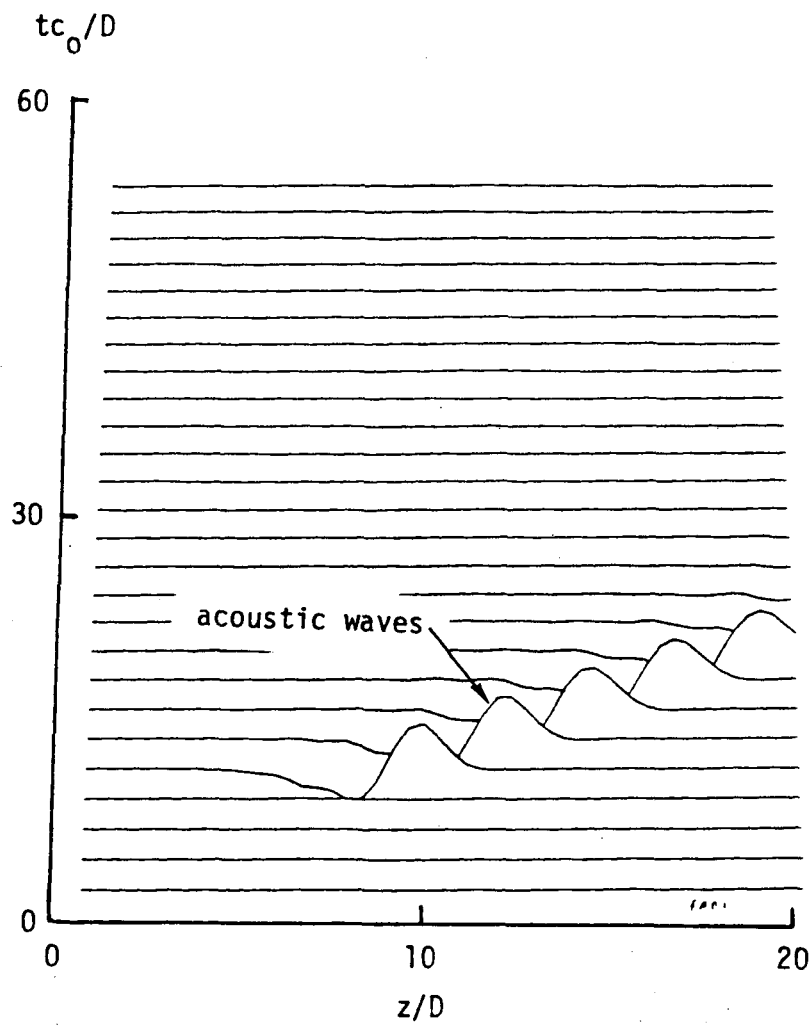


Figure 10. Three-dimensional prospective of the acoustic pulse (without flow) at $r/D = 0$.

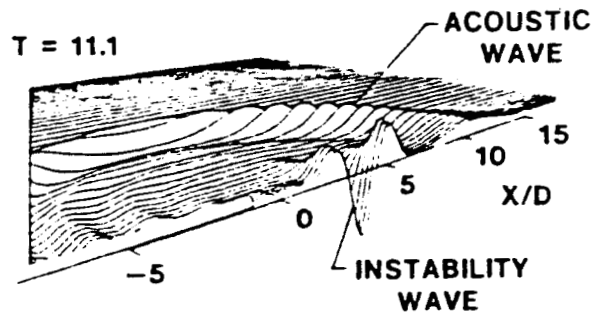


Figure 11a. Perspective plots of the fluctuating pressure.

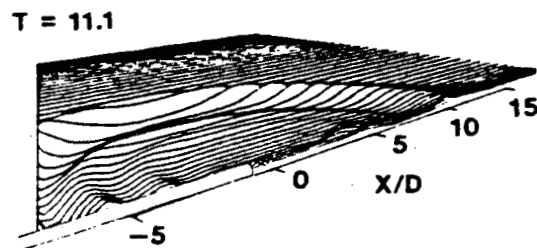


Figure 11b. Perspective plots of the fluctuating pressure without shear terms.

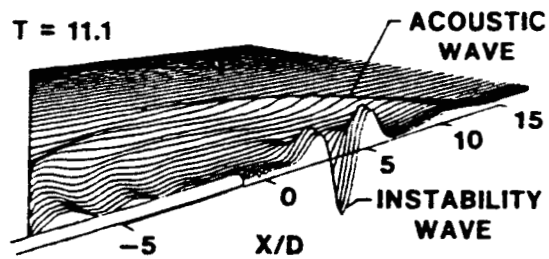


Figure 11c. Difference due to shear terms.

LIST OF FIGURES

- Figure 1. Computational domain.
- Figure 2. Mean velocity profile and radial derivative at $z/D = 2$.
- Figure 3a. Normalized R.M.S. velocity across the shear layer at $z/D = 2$.
- Figure 3b. Normalized R.M.S. velocity across the shear layer at $z/D = 4.2$.
- Figure 4. Measurements of the mean fluctuating velocity for the unexcited jet at $z/D = 2.0$.
- Figure 5a. Normalized time average Reynolds stresses and vorticity.
 $z/D = 2$.
- Figure 5b. Normalized time average Reynolds stresses and vorticity.
 $z/D = 4.2$.
- Figure 6. Centerline amplification rate of the longitudinal fluctuating velocity.
- Figure 7. Near-field amplification rate.
- Figure 8. Experimental near-field pressure with downstream distance.
- Figure 9a. Three-dimensional prospective of the evolution of the pressure amplitude at $r/D = 0$.
- Figure 9b. Three-dimensional prospective of the evolution of the pressure amplitude at $r/D = .4$.
- Figure 9c. Three-dimensional prospective of the evolution of the pressure amplitude at $r/D = .86$.
- Figure 9d. Three-dimensional prospective of the evolution of the pressure amplitude at $r/D = 1.5$.
- Figure 9e. Three-dimensional prospective of the evolution of the pressure amplitude at $r/D = 2.3$.
- Figure 9f. Three-dimensional prospective of the evolution of the pressure amplitude at $r/D = 3.3$.
- Figure 10. Three-dimensional prospective of the acoustic pulse (without flow) at $r/D = 0$.
- Figure 11a. Perspective plots of the fluctuating pressure.
- Figure 11b. Perspective plots of the fluctuating pressure without shear terms.
- Figure 11c. Difference due to shear terms.